Kasetsart J. (Nat. Sci.) 48 : 729 - 739 (2014)

Study of Stress Distribution in the Tibia During Stance Phase Running Using the Finite Element Method

Thepwachara Ruchirabha[1], Tumrong Puttapitukporn[1,*] and Siriporn Sasimontonkul[2]

ABSTRACT

Tibia fractures are common in the elderly who have osteoporosis. Stress distributions in the tibia of two osteoporosis patients were studied to investigate the cause of this fracture and the effects of contact areas on the distal end of the tibia, body weight and knee flexion angles on the tibial stresses were determined using finite element analysis. Three-dimensional tibial models were constructed from computed tomography images of legs using the Mimics V.10.01 program and the Geomagic V.10 program. These models were imported to the Catia V.5 program to perform the finite element analysis for determining stress distributions in the tibia.

The finite element models showed that the maximum von Mises stress found on the tibia of the female patient was higher than in the male patient since the contact area on the distal end of the female was smaller than in the male. Furthermore, the maximum von Mises stress occurred near the middle of the posterior tibia at 30º knee flexion and was slightly shifted toward the medial tibia during 30–90º knee flexion. As body weight increased, the maximum von Mises stress also increased. Moreover, the maximum von Mises stresses obtained from the smaller contact area were 17.6–25.2% (for a female patient) and 14.5–19.9% (for a male patient) higher than those determined from a larger contact area.

Keywords: tibia, computed tomography images, finite element analysis, osteoporosis

INTRODUCTION

Brittle bones are a common problem among the elderly with osteoporosis and can easily lead to bone fracture (National Institute of Health, 2014). Computed tomography (CT) images and the finite element method have been used to observe stress distribution in the bone. Khampagdee (2010) analyzed the stress in the head of an osteonecrotic hip joint using the finite element method in the Cosmos program. Sasimontonkul *et al*. (2007) reported that running led to the occurrence of maximal compressive and posterior shear forces applied to the distal end of the tibia at mid stance, which related to stress fracture of the tibia.

The objectives of this research were to observe stress distributions in the tibia during the stance phase of running and to determine the effects of contact area on the distal end of the tibia, body weight and knee flexion angles on tibia stresses using finite element analysis. Three-dimensional finite element models (FEMs)

1 Department of Mechanical Engineering, Faculty of Engineering, Kasetsart University, Bangkok 10900, Thailand.
2 Program in Sports Biomechanics, Faculty of Sports Science, Kasetsart University, Bangkok 10900, Thailand.
* Corresponding author, e-mail: fengtop@ku.ac.th

Received date : 25/03/14 Accepted date : 24/07/14

of the tibia consisting of cortical and cancellous bones based on the CT images of two osteoporosis patients were constructed using the Mimics V.10.01 (Materialise; Leuven, Belgium), the Geomagic V.10 (3D Systems; Rock Hill, SC, USA), and the Catia V.5 (Dassault Systèmes; Waltham, MA, USA) programs. Two contact areas on the distal end of the tibia were modeled according to the studies of Kura *et al.* (1998) and Wan *et al.* (2006). Kura *et al.(*1998) reported on the contact area of the ankle joint with axial loading and in positions of maximal dorsiflexion, plantar flexion, supination and pronation, while Wan *et al.* (2006) estimated an *in vivo* articular cartilage contact area of the human talocrural joint during the simulated stance phase of walking. The applied loads at the distal end of the tibia determined by Sasimontonkul *et al.* (2007) were used. The fixed areas on medial and lateral condyles were modeled according to the study of Eisenhart-Rothe *et al*. (2003) who found that contact areas of the patello-femoral and tibio-femoral joints depended on knee flexion angles.

MATERIAL AND METHODS

Validated model

To validate the accuracy of the FEM method in the Catia program, a cantilever beam was modeled consisting of a solid cylinder (50 mm diameter and 300 mm length) as shown in Figure 1. The FEM was formed using 1,9751 tetrahedral elements. The loads applied to the free end were a compressive force of 400 N and a shear force of 200 N. The material properties were Young's modulus of 70 GPa and Possion's ratio of 0.346.

Three-dimensional tibial models

The CT images of the legs of two osteoporosis patients (a 38 year-old male and a 64 year-old female) were used to create the three-dimensional tibial models. The CT images were imported into the Mimics V.10.01 program to erase irrelevant bones and to correct the right tibial surfaces consisting of cortical and cancellous bones as shown in Figures 2 and 3. Then, those tibial surfaces were repaired using the Geomagic V.10 program. Figures 4 and 5 show the repaired surfaces of the tibial bones of the female patient and male patient, respectively. Finally, the Catia V.5 program was used to create the assembly modeling of cortical and cancellous bones as shown in Figure 6.

Finite element modeling

The FEM of the right tibia consisted of cortical and cancellous bones. Twenty-four case studies were investigated to determine the effects of contact areas on the distal end of the tibia, bodyweight and knee flexion angles on tibial stresses as shown in Table 1. These FEMs were formed by tetrahedral elements in which the numbers of elements were tested to obtain the accurate results shown in Table 2. Contact surfaces without friction were constructed between the inner surface of the cortical bone and the outer surface of the cancellous bone.

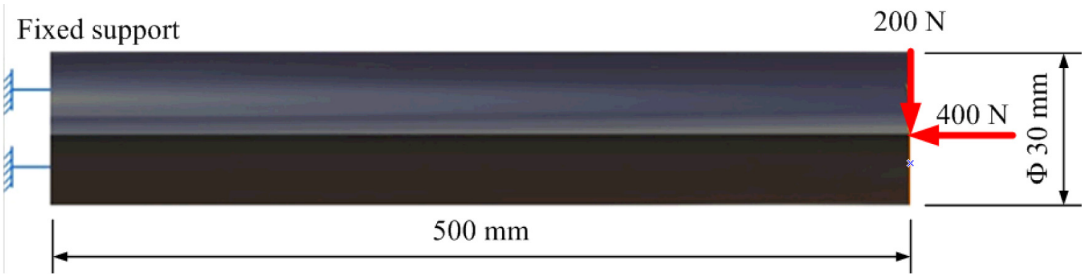

Figure 1 Validated model.

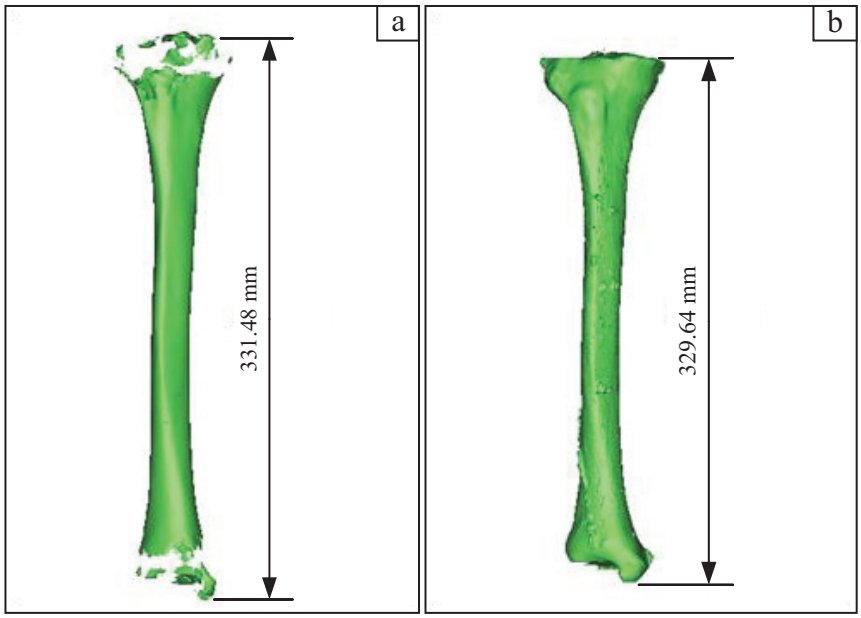

Figure 2 Computed tomography scan images of the tibial bone of a female patient: (a) Cortical bone; (b) Cancellous bone.

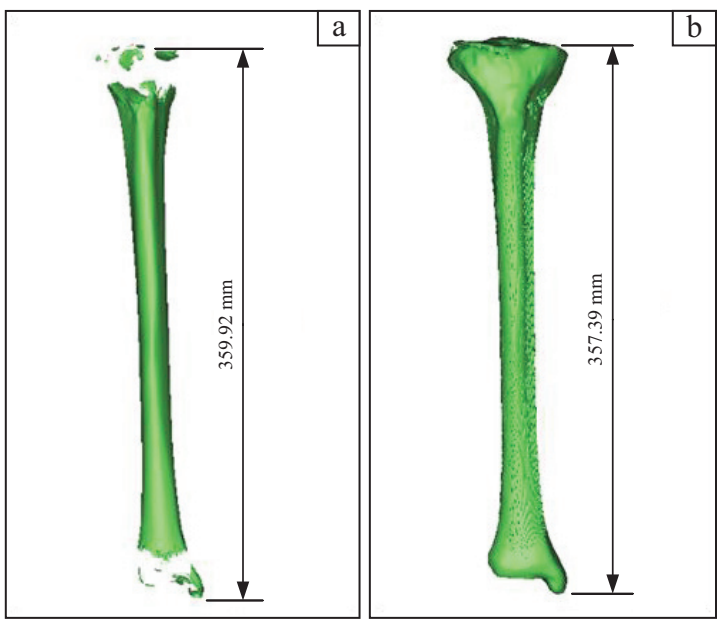

Figure 3 Computed tomography scan images of the tibial bone of a male patient: (a) cortical bone and (b) cancellous bone.

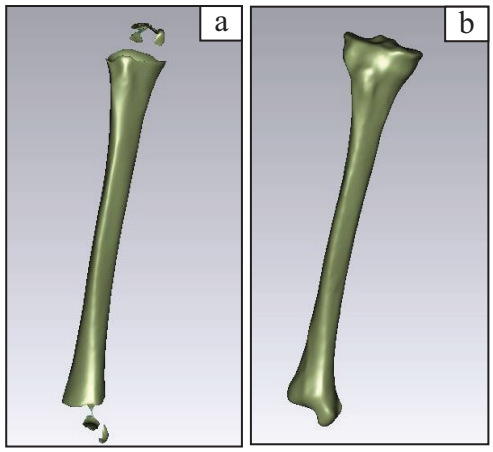

Figure 4 Repaired surfaces of the tibial bone of a female patient: (a) Cortical bone; (b) Cancellous bone.

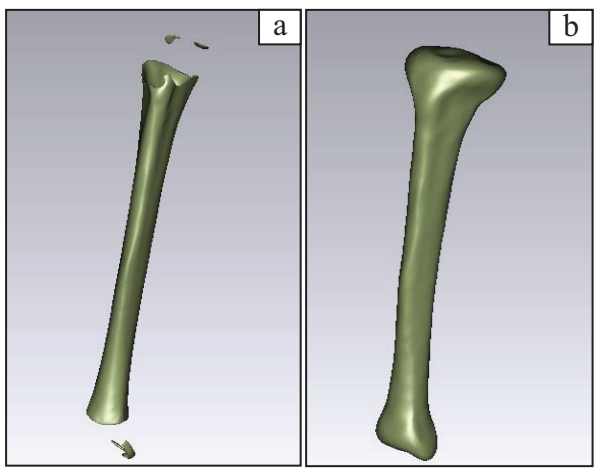

Figure 5 Repaired surfaces of the tibial bone of a male patient: (a) Cortical bone; (b) Cancellous bone.

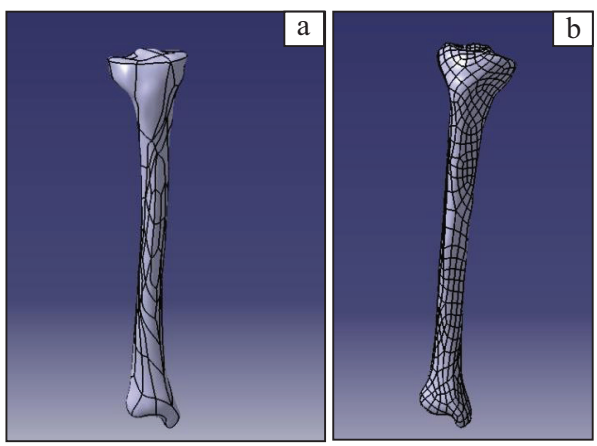

Figure 6 Three-dimensional tibial models consisting of cortical and cancellous bones: (a) Female patient; (b) Male patient**.**

Table 1 Case studies classified by contact areas on the distal end of the tibia, knee flexion angles and body weight.

Case study number	Patient		Contact area (distal end)		Knee flexion angle (°)		Body weight (kg)		
	Female	Male	Kura *et al*. (1998)	Wan *et al*. (2006)	30º	30–90º	40	60	80
1	√		√		√		√		
2	√		√		√			√	
3	√		√		√				√
4	√		√			√	√		
5	√		√			√		√	
6	√		√			√			√
7	√			√	√		√		
8	√			√	√			√	
9	√			√	√				√
10	√			√		√	√		
11	√			√		√		√	
12	√			√		√			√
13		√	√		√		√		
14		√	√		√			√	
15		√	√		√				√
16		√	√			√	√		
17		√	√			√		√	
18		√	√			√			√
19		√		√	√		√		
20		√		√	√			√	
21		√		√	√				
22		√		√		√	√		
23		√		√		√		√	
24		√		√		√			√

Table 2 Number of nodes and elements used in the finite element models.

Case study	Number of nodes	Number of elements
1–3	3,493	14,050
4–6	3,500	14,089
7–9	3,483	14,015
10–12	3,493	14,056
13–15	3,441	12,844
16–18	3,449	12,937
19–21	3,452	12,932
22–24	3,443	12,888

Material properties

The material properties of the cortical and cancellous bones obtained from Reilly and Burstein (1975) and Pacific Research Laboratories (2002) are provided in Table 3.

Boundary conditions

The contact areas on the distal end of the tibia were modeled according to the studies of Kura *et al.* (1998) and Wan *et al.* (2006). Figure 7 shows these contact areas on the distal end of the FEMs specified by Kura *et al.* (1998) which were 206.6 mm^2 for a female and 307.6 mm^2 for a male. Figure 8 shows the contact areas on the distal end of the FEMs specified by Wan *et al.* (2006) which were 151.9 mm^2 (39.93% of the articular surface) for a female and 266.6 mm^2 (41.41% of the articular surface) for a male. Thereafter, compressive and posterior shear forces estimated from three body weights consisting of 40, 60 and 80 kg from Sasimontonkul *et al.*(2007) were applied to the FEM to observe the effect of weight bearing (Table 4). The fixed contact areas on the proximal end of tibias were modeled according to the study of Eisenhart-Rothe *et al.* (2003). Figure 9 shows these fixed contact areas which totaled 71.87 mm^2 for both female and male patients. At 30^o knee flexion, the centroids of the fixed contact

Table 3 Material properties of tibial bones (Reilly and Burstein, 1975; Pacific Research Labs Inc. (2002).

Bone type	Young's modulus (GPa)	Poisson ratio	Density ($kg.m^{-3}$)
Cortical bone	6.90	0.25	1,700
Cancellous bone	1.00	0.30	270

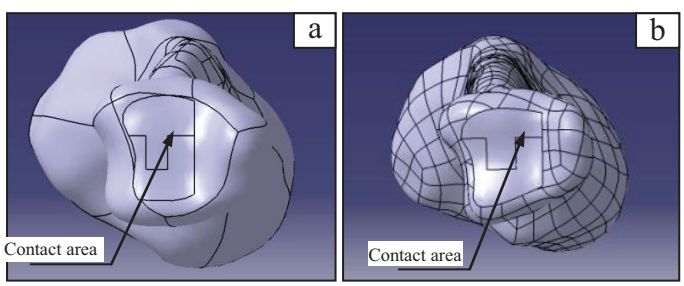

Figure 7 Contact areas on the distal end of tibia specified by Kura *et al*. (1998): (a) Female patient; (b) Male patient.

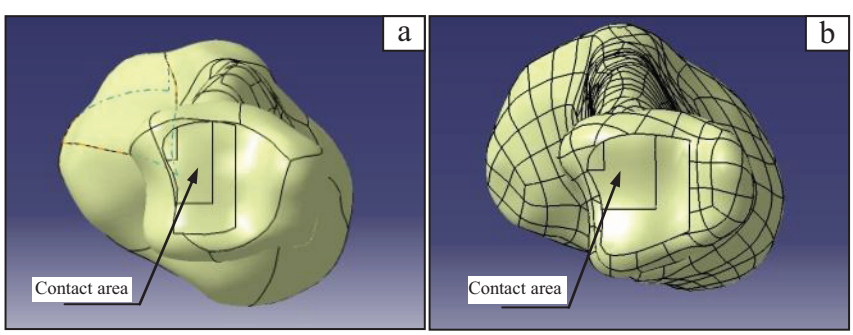

Figure 8 Contact areas on the distal end of tibias specified by Wan *et al*. (2006): (a) Female patient; (b) Male patient.

areas were 3.2 mm below the centroid of the medial condyle and 2.2 mm above the centroid of the lateral condyle. During 30–90º knee flexion, the centroids of the fixed contact areas were 0.9 mm below the centroid of the medial condyle and 3.5 mm above the centroid of the lateral condyle.

RESULTS

Figure 10 shows the contour plot of von Mises stress of the validated model. The maximum von Mises stress found at the fixed end was 9.06 MPa which yielded an error of less than 1.3%. Figure 11 shows the plot of maximum von Mises stress versus the number of elements for a female patient (case study 5) and a male patient (case study 17) to validate the FE models. It was found that the numbers of elements in the FEMs were greater than 14,000 elements for the tibial bone of the female patient while there were 12,800 elements for the tibial bone of the male patient. The maximum von Mises stresses for case studies 1–24 are shown in Tables 5 and 6. Figures 12 and 13 show the von Mises stress distributions on the tibial surfaces for case studies 1–24.

DISCUSSION

The FEMs show that the case studies with the contact area specified by Wan *et al*. (2006) yielded higher maximum von Mises stresses than ones with the contact area specified by Kura *et al.* (1998). This might have resulted from the fact that the contact areas of Wan *et al.* (2006) were smaller than those of Kura *et al.* (1998). Moreover,

Table 4 Applied forces on the contact area on the distal end of the tibia.

Body weight (kg)	Compression force (N)	Posterior shear force (N)
40	3,496.284	207.972
60	5,244.426	311.958
80	6,992.568	415.944

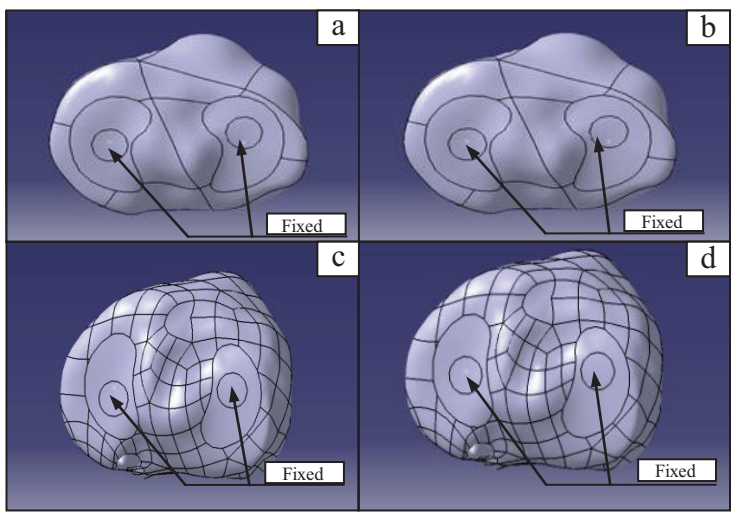

Figure 9 Fixed contact areas on the proximal end of tibia: (a) Female patient with 30º knee flexion; (b) Female patient with 30–90º knee flexion; (c) Male patient with 30º knee flexion; (d) Male patient with 30–90º knee flexion.

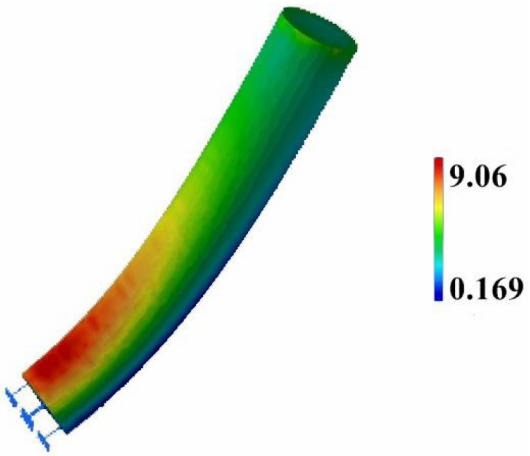

Figure 10 Contour plot of the von Mises stress distribution (MPa) in the validated model.

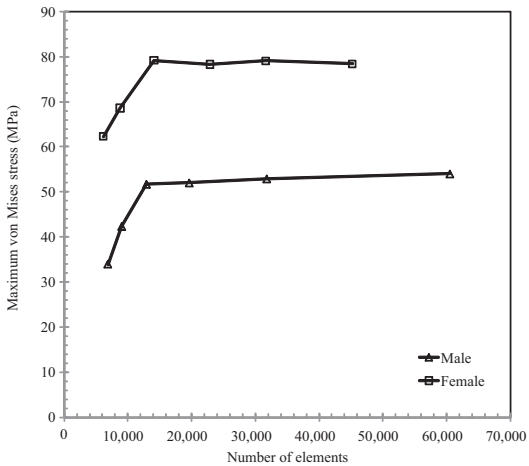

Figure 11 Number of elements versus maximum von Mises stress for female patient (case study 5) and male patient (case study 17) with the contact area specified by Kura et al. (1998), 30–90° knee flexion, and 60–80 kg body weight.

Table 5 Maximum von Mises stresses at 30° knee flexion for different male and female body weights.

Body weight (kg)	Maximum von Mises stress (MPa)			
	Kura *et al.* (1998)		Wan *et al.* (2006)	
	Female	Male	Female	Male
40	48.3	34.6	56.8	41.5
60	72.4	51.9	85.2	62.2
80	96.5	69.2	114.0	83.0

Table 6 Maximum von Mises stresses during 30°-90° knee flexion different male and female body weights.

Body weight (kg)	Maximum von Mises stress (MPa)			
	Kura *et al*. (1998)		Wan *et al*. (2006)	
	Female	Male	Female	Male
40	52.8	34.4	66.1	40.4
60	79.2	51.7	99.2	59.2
80	106.0	68.9	132.0	80.8

the maximum von Mises stress found on the tibia of the female patient was higher than on the male patient since the contact area on the distal end of the female was smaller than on the male. For the case studies with 30° knee flexion, the maximum von Mises stresses were found at the middle of the posterior tibia. However, for the case studies with 30–90° knee flexion, the location of the maximum von Mises stresses shifted a little more toward the medial tibia. As the body weight increased, the maximum von Mises stress increased. For a male patient, the knee flexion angle had little impact on the maximum von Mises stress. However, for a female patient, the maximum von Mises stress increased as the knee angle increased.

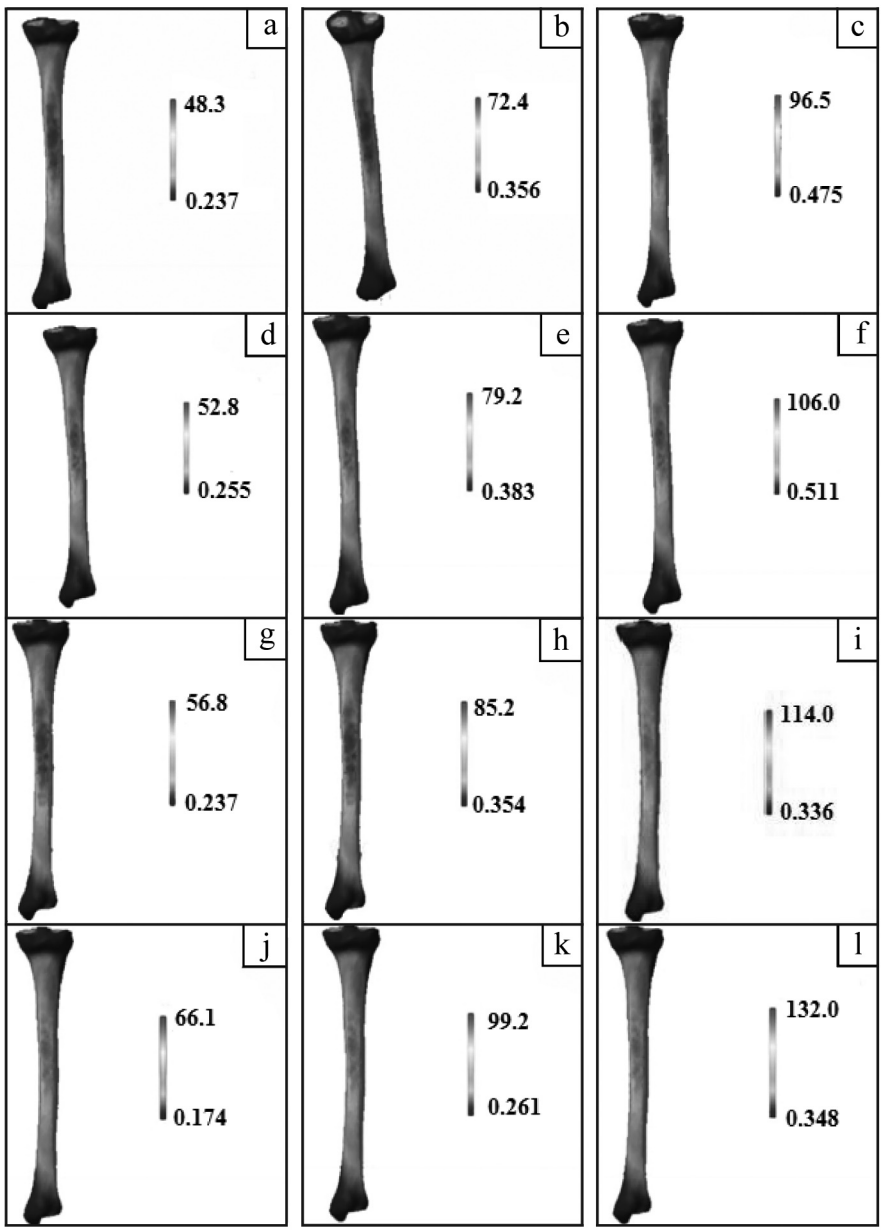

Figure 12 Von Mises stress distribution (MPa) on tibial surface of female patient for case studies a–l.

CONCLUSION

The tibia models consisting of cortical and cancellous bones were successfully constructed using CT images. The stress distributions in the tibia of two osteoporosis patients were studied using FEM analyses. It was found that the maximum von Mises stress occurred near the middle of the posterior tibia. The maximum von Mises stress found on the tibia of the female patient was higher than for the male patient. As the body weight increased, the maximum von Mises stress increased. Moreover, the FEM using the contact area specified by Wan *et al.* (2006) resulted in 17.6–25.2% (female patient) and 14.5–19.9% (male patient) greater maximum von Mises stress compared with using contact areas specified by Kura *et al.* (1998).

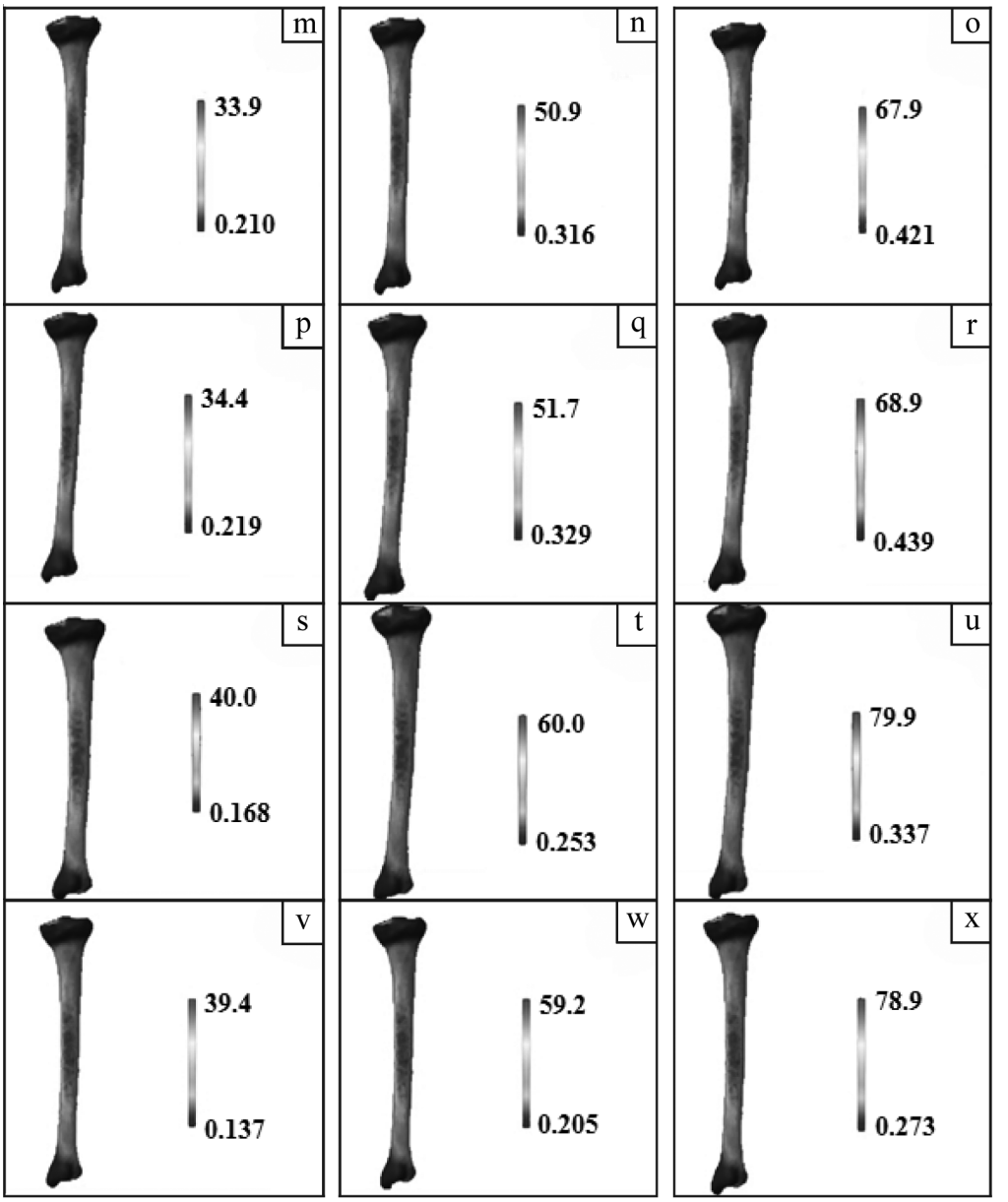

Figure 13 Von Mises stress distribution (MPa) on tibial surface of male patient for case studies m–x.

ACKNOWLEDGEMENTS

The authors acknowledged Phramongkutklao Hospital for the kind provision of CT images and National and Material Technology Center (MTEC) for the use of the software programs.

LITERATURE CITED

Eisenhart-Rothea R.V., M. Siebertb, C. Bringmannb, T. Vogl, K.H. Englmeier and H. Graichen. 2003. A new *in vivo* technique for determination of 3D kinematics and contact areas of the patello-femoral and tibio-femoral joint. **J. Biomech. Eng.** 37: 927–934.

Khampakdee. M. 2010. **Analysis of the Stress on Femoral Head Ischemia Using Finite Element Method.** MSc thesis, Srinakharinwirot University, Bangkok, Thailand.

Kura, H., H.B. Kitaoka, Z.P. Luo. And K. A. An. 1998. Measurement of surface contact area of the ankle joint. **Clin. Biomech.** 13: 365–370.

National Institute of Health. 2014. **Osteoporosis.** [Available from: http://www.nlm.nih.gov/medlineplus/osteoporosis.html]. [Sourced: 6 August 2014]

Pacific Research Labs Inc. 2002. **Biomechanical Testing Material.** [Available from: http://secure.sawbones.com/product/bio/composite.asp]. [Sourced: 3 April 2002].

Reilly, D.T. and A.H. Burstein, 1975. The elastic and ultimate properties of compact bone tissue. **J. Biomech. Eng.** 8: 393–405.

Sasimontonkul, S. B.K. Bay and M.J. Pavol. 2007. Bone contact forces on the distal tibia during the stance phase of running. **J. Biomech. Eng.** 40(15): 3503–3509.

Wan. L, R.J. de Asla, H.E. Rubash and G.Li. 2006. Determination of *in-vivo* articular cartilage contact areas of human talocrural joint under weight-bearing conditions. **Osteoarthritis and Cartilage** 14: 1294–1301.